

1

Untwisting the Boerdijk–Coxeter Helix

2

Robert L. Read read.robert@gmail.com

3

4 **Abstract.** The Boerdijk–Coxeter helix (BC helix, or tetrahelix) is a face-to-face stack of regular tetrahedra
 5 forming a helical column. Considering the edges of these tetrahedra as structural members, the
 6 resulting structure is attractive and inherently rigid, and therefore interesting to architects, me-
 7 chanical engineers, and robotocists. A formula is developed that matches the visually apparent
 8 helices forming the outer rails of the BC helix. This formula is generalized to a formula conve-
 9 nient to designers. Formulae for computing the parameters that give edge-length minimax-optimal
 10 tetrahelices are given, defining a continuum of tetrahelices of varying curvature. The endpoints of
 11 the optimality of this continuum are the BC helix and a structure of zero curvature, the *equite-*
 12 *trabeam*. Numerically finding the rail angle from the equation for pitch allows optimal tetrahelices
 13 of any pitch to be designed. An interactive tool for such design and experimentation is provided:
 14 <https://pubinv.github.io/tetrahelix/>. A formula for the inradius of optimal tetrahelices is given.
 15 Utility for static and variable geometry truss/space frame design and robotics is discussed.

16

Key words. Boerdijk–Coxeter helix, tetrahelix, robotics, tetrobot, unconventional robots, structural engineer-
 17 ing, mechanical engineering, tensegrity, variable-geometry truss

18

AMS subject classifications. 51M15

19

1. Introduction. The Boerdijk–Coxeter helix[3] (BC helix), is a face-to-face stack of tetra-
 20 hedra that winds about a straight axis. Because architects, structural engineers, and roboto-
 21 cists are inspired by and follow such regular mathematical models but can also build struc-
 22 tures and machines of differing or even dynamically changing length, it is useful to develop
 23 the mathematics of structures formed from tetrahedra where we relax regularity.

24

The vertices of the tetrahedra lie upon three helices about the central axis. The glussbot[11] (or Tetrobot)[8] uses the regularity of this geometry to make a tentacle-like robot that can crawl like a slug or mollusc. The Tetrobot uses mechanical actuators which can change their length, connected by special joints, such as the 3D printable Song-Kwon-Kim[15] joint, or the CMS joint[7] which allow many members to meet in a single point. Such machines can follow purely regular mathematical models such as the Boerdijk–Coxeter helix or the Octet Truss[4].

30

Buckminster Fuller called the BC helix a *tetrahelix*[5], a term now commonly used. In this paper we reserve *BC helix* to mean the purely regular structure and use *tetrahelix* to refer to any structure isomorphic to the BC helix.

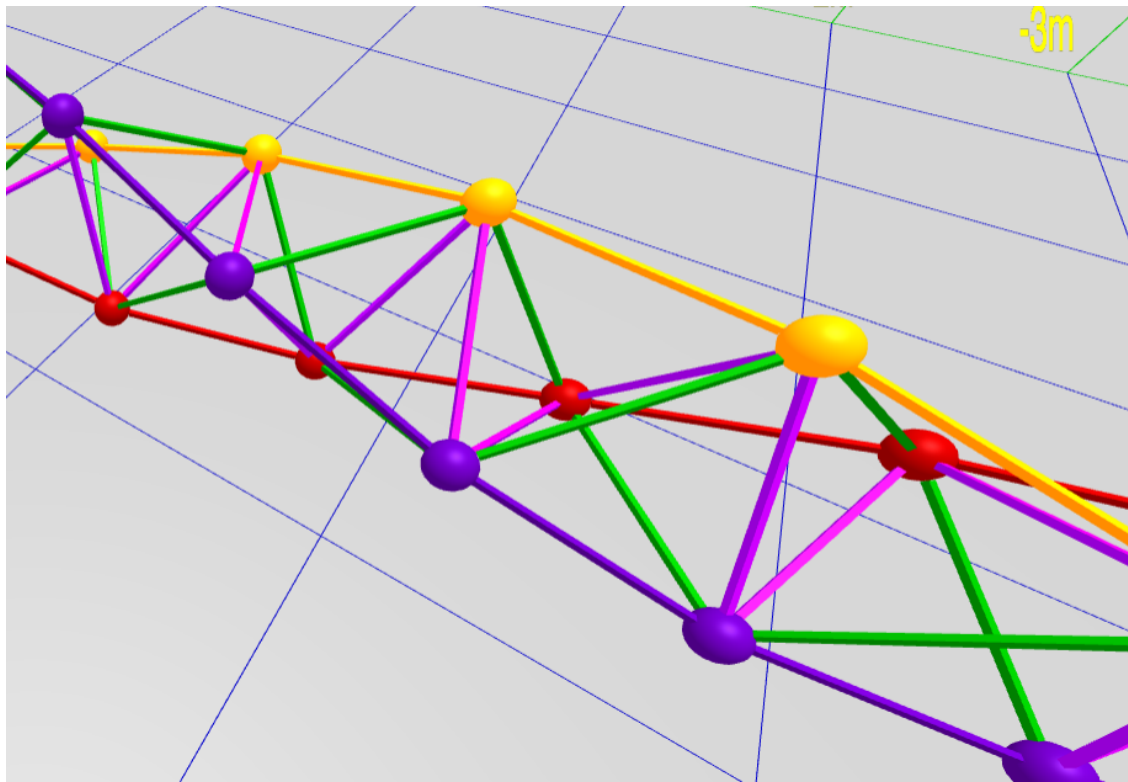


Figure 1. BC Helix Close-up (partly along axis)

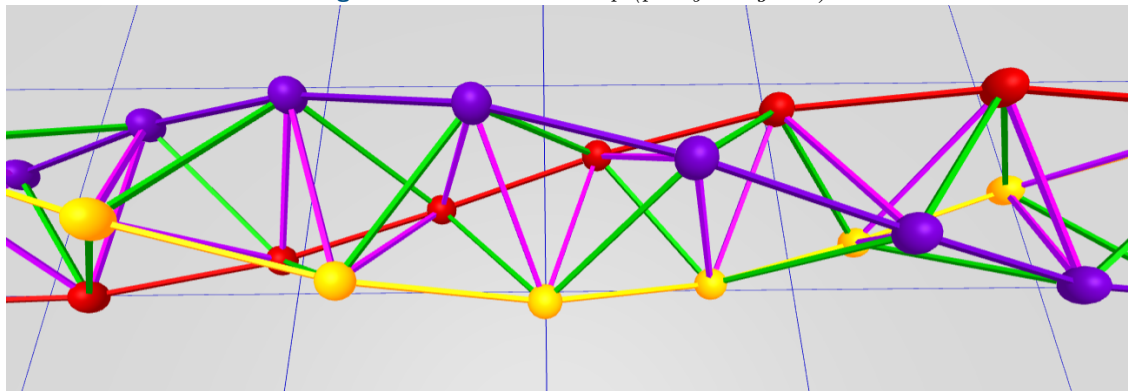


Figure 2. BC Helix Close-up (orthogonal)

33 Imagining Figure 2 as a static mechanical structure, we observe that it is useful to the
 34 mechanical engineer or robotocist because the structure remains an inherently rigid, omni-
 35 triangulated space frame, which is mechanically strong. Imagine further in Figure 2, that each
 36 static edge was replaced with an actuator that could dynamically become shorter or longer in
 37 response to electronic control, and the vertices were a joint that supported sufficient angular
 38 displacement for this to be possible. An example of such a machine is a glussbot, shown in
 39 Figure 11.

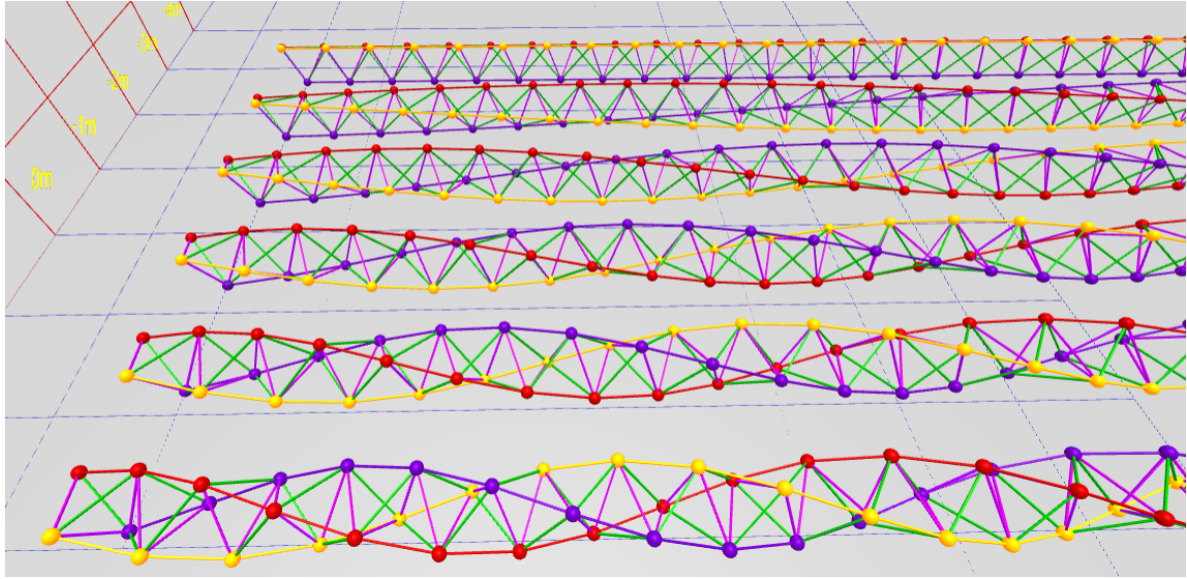


Figure 3. A Continuum of Tetrahelices

40 A BC helix does not rest stably on a plane. It is convenient to be able to “untwist” it and
 41 to form a tetrahelix space frame that has a flat planar surface. By making length changes in a
 42 certain way, we can untwist a tetrahelix to form a *tetrabeam* which has planar faces and has,
 43 for example, an equilateral triangular profile. This paper develops the equations needed to
 44 untwist the tetrahelix. All math developed here is available in JavaScript and demonstrated
 45 by an interactive design website <https://pubinv.github.io/tetrahelix/>[12], from which Figure 2
 46 and the figures below are taken.

47 Figure 3 displays a continuum of tetrahelices optimal in a certain sense, which is the result
 48 of this paper. The closest helix is the BC helix, and the furthest is the equitetrabeam, defined
 49 in section 6.

50 **2. A Designer’s Formulation of the BC Helix.** We would like to design nearly regular
 51 tetrahelices with a formula that gives the vertices in space. Eventually we would like to design
 52 nearly regular tetrahelices by choosing the lengths of a small set of members. In a space frame,
 53 this is a static design choice; in a tetrobot, it is a dynamic choice that can be used to twist
 54 the robot and/or exert linear or angular force on the environment.

55 Ideally we would have a simple formula for defining the nodes based on any curvature
 56 or pitch we choose. It is a goal of this paper to relate these two approaches to generating a
 57 tetrahelix continuum.

58 H.S.M Coxeter constructs the BC helix[3] as a repeated rotation and translation of the
 59 tetrahedra, showing the rotation is:

$$60 \quad \theta_{bc} = \arccos(-2/3)$$

61 and the translation:

62
$$h_{bc} = 1/\sqrt{10}$$

63 θ_{bc} is approximately $0.37 \cdot 2\pi$ radians or 131.81 degrees. The angle θ_{bc} is the rotation of
64 each tetrahedron, not the tetrahedra along a rail. In [Figure 2](#), each tetrahedron has either a
65 yellow, blue, or red outer edge or rail. That is, a blue-rail tetrahedron is rotated slightly more
66 than a $1/3$ of a revolution to match the face of the yellow tetrahedra.

67 R.W. Gray's site[\[6\]](#), repeating a formula by Coxeter[\[3\]](#) in more accessible form, gives the

68 Cartesian coordinates $\begin{bmatrix} x \\ y \\ z \end{bmatrix}$ for a counter-clockwise BC Helix:

69 (1)
$$V(n) = \begin{bmatrix} r_{bc} \cos n\theta_{bc} \\ r_{bc} \sin n\theta_{bc} \\ nh_{bc} \end{bmatrix}, \text{ where: } \begin{aligned} r_{bc} &= \frac{3\sqrt{3}}{10} \approx 0.5196 \\ h_{bc} &= 1/\sqrt{10} \approx 0.3162 \\ \theta_{bc} &= \arccos(-2/3) \end{aligned}$$

70 where n represents each integer numbered node in succession on every colored rail.

71 The apparent rotation of a vertex an outer-edge, $V(n)$ relative from $V(n+3)$ for any
72 integer n in (1), is $3\theta_{bc} - 2\pi$.

73 This formula defines a helix, but it is not any of the apparent helices, or *rail* helices, of the
74 BC helix, but rather one that winds three times as rapidly through all nodes. To a designer of
75 tetrahelices, it is more natural to think of the three helices which are visually apparent, that
76 is, those three which are closely approximated by the outer edges or rails of the BC helix. We
77 think of each of these three rails as being a different color: red, blue, or yellow. This situation
78 is illustrated in [Figure 4](#), wherein the black helix represents that generated by (1), and the
79 colored helices are generated by (2).

80 In order to develop the continuum of slightly irregular tetrahelices described in [section 7](#),
81 we need a formula that gives us the nodes of just one rail helix, denoted by color c and integer
82 node number n :

83
$$(\forall n \in \mathbb{Z}, \forall c \in \{0, 1, 2\} : H_{BCcolored}(n, c) = V(3n + c))$$

84 Such a helix can be written:

85 (2)
$$H_{BCcolored}(n, c) = \begin{bmatrix} r_{bc} \cos ((3\theta_{bc} - 2\pi)n + c\theta_{bc}) \\ r_{bc} \sin ((3\theta_{bc} - 2\pi)n + c\theta_{bc}) \\ 3h_{bc}(n + c/3) \end{bmatrix}, \text{ where } \begin{aligned} r_{bc} &= \frac{3\sqrt{3}}{10} \\ h_{bc} &= 1/\sqrt{10} \\ \theta_{bc} &= \arccos(-2/3) \end{aligned}$$

86 In this formula, integral values of n may be taken as a node number for one rail and
87 used to compute its Cartesian coordinates. Allowing n to take non-integer values defines a
88 continuous helix in space which is close to the segmented polyline of the outer tetrahedra
89 edges, and equals them at integer values.

90 [Figure 4](#) illustrates this difference with a 7-tetrahedra BC helix, which is in fact the same
91 geometry as the robot illustrated in [Figure 11](#). Although the nodes coincide, (1) evaluated
92 at real values generates the black helix which runs through every node, and (2) defines the
93 red, yellow, and blue helices. (In this figure these rail helices have been rendered at a slightly

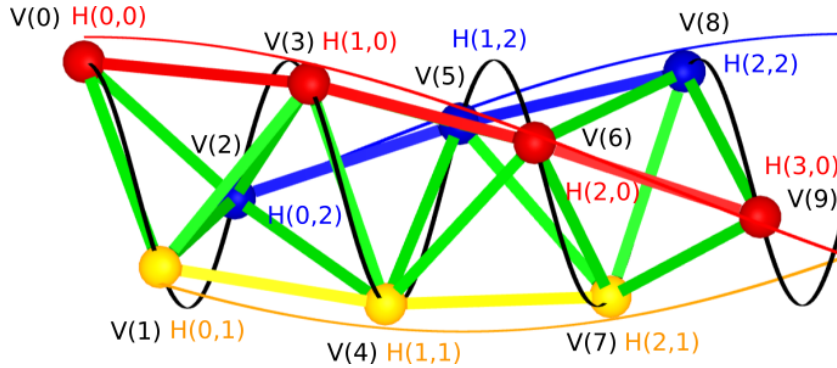


Figure 4. Rail helices (H) vs. Coxeter/Gray helix (V)

higher radius than the nodes for clarity; in actuality the maximum distance between the continuous, curved helix and the straight edges between nodes is much smaller than can be clearly rendered.)

The quantity $(3\theta_{bc} - 2\pi) \approx 35.43^\circ$ is the angular shift between $V(3n+c) = H_{BCcolored}(n, c)$ and $V(3(n+1)+c) = H_{BCcolored}(n+1, c)$. This quantity appears so often that we call it the “rail angle ρ ”. For the BC helix, $\rho_{bc} = (3\theta_{bc} - 2\pi)$.

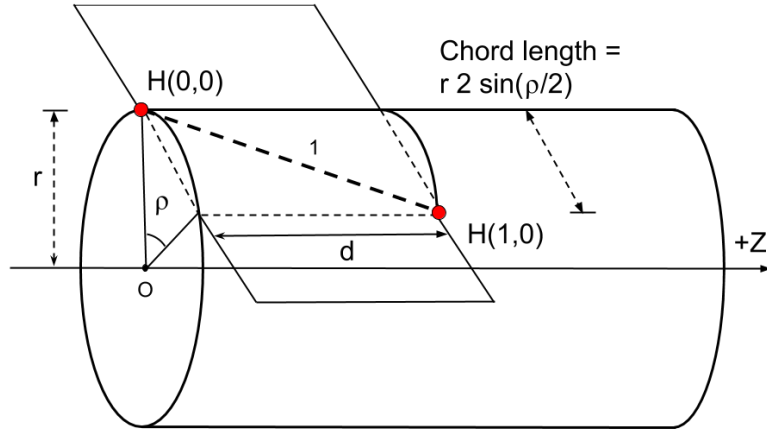


Figure 5. Rail Angle Geometry

Note in Figure 5 the z -axis travel for one rail edge is denoted by d . In (1) and (2), the variable h is used for one third of the distance we name d . We will later justify that $d = 3h$. In this paper we assume the length of a rail is always 1 as a simplification, except in proofs concerning rail length. (We make the rail length a parameter in our JavaScript code

104 in https://github.com/PubInv/tetrahelix/blob/master/js/tetrahelix_math.js [12].)

105 The $H_{BCcolored}(n, c)$ formulation can be further clarified by rewriting directly in terms of
106 the rail angle ρ_{bc} rather than θ_{bc} . Intuitively we seek an expression where $c/3$ is multiplied by
107 a $1/3$ rotation plus the rail angle ρ . We expand the expressions θ_{bc} and ρ_{bc} in (2) and seek to
108 isolate the term $c2\pi/3$.

$$\begin{aligned} 109 \quad c\theta_{bc} &= \{\text{we aim for } 3 \text{ in denominator, so we split...}\} \\ 110 \quad (c/3)(3\theta_{bc}) &= \{\text{we want } 2\pi \text{ in numerator, so add canceling terms...}\} \\ 111 \quad (c/3)((3\theta_{bc} - 2\pi) + 2\pi) &= \{\text{definition of } \rho_{bc}\}... \\ 112 \quad (c/3)\rho_{bc} + c2\pi/3 &= \{\text{algebra...}\} \\ 113 \quad c(\rho_{bc} + 2\pi)/3 & \\ 114 \end{aligned}$$

116 This allows us to redefine:

$$117 \quad (3) \quad H_{BCcolored}(n, c) = \begin{bmatrix} r \cos \rho_{bc} n + c(\rho_{bc} + 2\pi)/3 \\ r \sin \rho_{bc} n + c(\rho_{bc} + 2\pi)/3 \\ (n + c/3)h_{bc} \end{bmatrix}, \text{ where } \begin{aligned} \rho_{bc} &= (3\theta_{bc} - 2\pi) \\ h_{bc} &= 1/\sqrt{10} \end{aligned}$$

118 Recall that $c \in \{0, 1, 2\}$, but n is continuous (rational or real-valued.) We can now assert
119 that in Figure 4 the black helix winds at $\frac{3\theta_{bc}}{\rho_{bc}} \approx 11.16$ times the rate of a rail helix.

120 From this formulation it is easy to see that moving one vertex on a rail ($H_{BCcolored}(n, c)$)
121 to $H_{BCcolored}(n + 1, c)$ for any n and c) moves us ρ_{bc} radians around a circle. Since:

$$122 \quad \frac{2\pi}{\rho_{bc}} \approx 10.16$$

123 we can see that there are approximately 10.16 red, blue or yellow tetrahedra on one rail in a
124 single revolution.

125 The *pitch* of any tetrahelix, defined as the axial length of a complete revolution where
126 $\rho \neq 0$ is:

$$127 \quad (4) \quad p(\rho) = \frac{2\pi \cdot d}{\rho}$$

128 The pitch of the Boerdijk–Coxeter helix of edge length 1 is the length of three tetrahedra
129 times this number:

$$130 \quad \frac{3h_{bc} \cdot 2\pi}{\rho_{bc}} = \frac{6\pi}{\sqrt{10}\rho_{bc}} \approx 9.64$$

132 The pitch is less than the number of tetrahedra because the tetrahedra are not lined
133 up perfectly. It is a famous and interesting result that the pitch is irrational. A BC helix
134 never has two tetrahedra at precisely the same orientation around the z -axis. However, this
135 is inconvenient to designers, who might prefer a rational pitch. The idea of developing a

136 rational period by arranging solid tetrahedra by relaxing the face-to-face matching has been
137 explored[13]. We develop below slightly irregular edge lengths that support, for example, a
138 pitch of precisely 12 tetrahedra in one revolution which would allow an architect to design a
139 column having a basis and a capital in the same relation to the tetrahedra they touch at the
140 bottom and top of the column.

141 **3. Optimal Tetrahelices are Triple Helices.** We use the term *tetrahelix* to mean any
142 structure made of vertices and edges which is isomorphic to the BC helix and in which the
143 vertices lie on three helices. We further demand that all edge lengths be finite, as we are only
144 interested in physically constructable tetrahelices. By isomorphic we mean there is a one-
145 to-one mapping between both vertices and edges in the two tetrahelices. One could consider
146 various definitions of optimality for a tetrahelix, but the most useful to us as robotocists
147 working with the Tetrobot concept is to minimize the maximum ratio between any two edge
148 lengths, because the Tetrobot uses mechanical linear actuators with limited range of extension.

149 A *triple helix* is three congruent helices that share an axis. We show that optimal tetra-
150 helices are in fact triple helices with the same radius, so that all vertices are on a cylinder.
151 In, stages, we demonstrate that optimal tetrahelices:

- 152 1. have the same pitch,
- 153 2. have parallel axes,
- 154 3. share the same axis,
- 155 4. have the same radius,
- 156 5. have the same rail lengths,
- 157 6. have axially equidistant nodes, and therefore
- 158 7. are in fact triple helices.

159 Suppose that all three rails do not have the same pitch. Starting at any shortest edge
160 between two rails, as we move from node to node away from our start edge the edge lengths
161 between rails must always lengthen without bound, which cannot be optimal. So we are
162 justified in talking about the *pitch* of the optimal tetrahelix as the pitch of its three rail
163 helices, even though there are three such helices of equivalent pitch.

164 Similarly, if the axes are not parallel, there is an edge of unbounded length in the structure,
165 so we do not consider such cases.

166 Define a *minimax edge-length optimal tetrahelix* or just an *optimal tetrahelix* to be a
167 tetrahelix for which there exists no other tetrahelix with lower ratio of longest edge length to
168 shortest edge length.

169 We wish to show that in an optimal tetrahelix, all vertices lie on the cylinder of radius r ,
170 regardless of where they lie on the z -axis.

171 As a little lemma for the proof below, observe that a tetrahelix of zero radius, where all
172 points lie on the same line, is not as optimal as a tetrahelix of a small radius. The edges
173 between rails will be shorter than the rail edges, and moving them apart slightly lengthens
174 the between-edge rails.

175 **Theorem 1.** *Any optimal tetrahelix with a rail angle of magnitude less than π has all three
176 axes coincident.*

177 *Proof.* Case 1: Suppose that ρ is zero. Then for any given inradius, the figure in the

178 XY -plane of an equilateral triangle is the minimax solution for all non-rail edges. Since all
 179 rail edges are of length 1, this is the minimax solution for the entire set. Since the vertices of
 180 an equilateral triangle lie on a circle, all points in three-space lie on a cylinder.

181 Case 2: Suppose that ρ is positive but less than π . In this case each rail helix has
 182 curvature. The projection of points in the XY plane creates a figure guaranteed to have
 183 point on either side of any line through the axis of such a helix, because the figure is either
 184 an n -gon or a circle. We show that the three helices share a common axis.

185 Without loss of generality define the Red helix to have its axis on the z -axis. Without
 186 loss of generativity define the Blue helix to be a helix that has an edge connection to the Red
 187 helix that is either a maximum or a minimum. Let B' be the blue helix translated in the
 188 XY -plane so that its axis is the z -axis and condicent with the red helix R . Let D be the
 189 distance between the axis of the Blue helix B and B' . We will show that if $D > 0$ then B
 190 “wobbles” in a way that cannot be optimal. Define a wobble vector by:

$$191 \quad W(n) = B(n) - B'(n)$$

192 where $B(n)$ is the cartesian vector $\begin{bmatrix} x \\ y \end{bmatrix}$ for the projection of the n th blue vertex. Note that
 193 $\|R(n) - B'(n+k)\|$ is a constant for any k , because R and B' have the same pitch and the
 194 same axis, even if they do not have the same radius (which we are currently proving.)

195 [Figure 6](#) demonstrates illustrates this situation. Like most diagrams, it is over specific,
 196 in that the two circles are drawn of the same radius but we do not depend upon that in this
 197 proof. The diagram represents the projection along the z axis of points into the XY -plane.

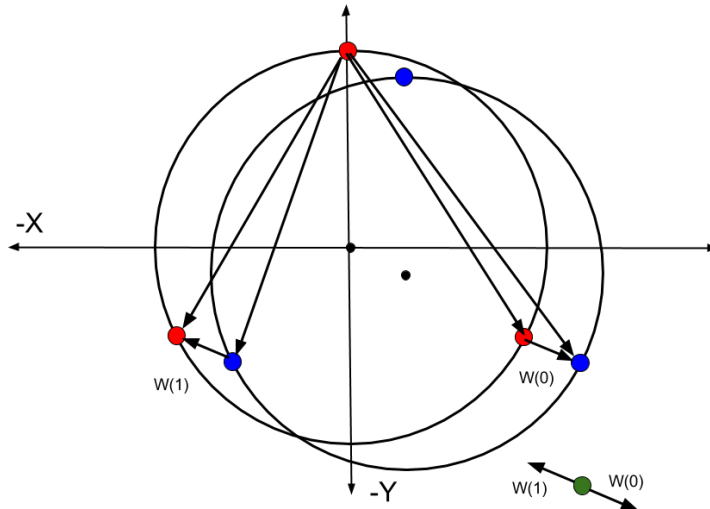


Figure 6. Wobble Vectors from Non-Coincident Axes

198 Since $-\pi < \rho < \pi$, each rail helix rotates about its axis as a function of n and defines at

199 least 3 unique points when projected onto the XY -plane around its axis. If $2\pi/\rho$ is irrational,
 200 it defines a circle. If $2\pi/\rho$ is rational it defines an n -gon in the XY -plane, where n is at least
 201 3 (when $\rho = 2\pi/3$). The set of wobbles $\{W(n)|\text{for any } n\}$ thus contains at least three vectors,
 202 pointing in different directions. For any point not at the origin, at least one of these vectors
 203 moves closer to the point and at least one moves further away.

204 The set of all lengths in the tetrahelix is a superset of: $L = \{\|R(n) - B(n)\|\}$, which by
 205 our choice has at least one longest or shortest length. $L = \{\|R(n) - (B'(n) + W(n))\|\}$ and
 206 so $L = \{\|(R(n) - B'(n)) - W(n)\|\}$. But $R(n) - B'(n)$ is a constant, so the minimax value of
 207 L is improved as $\|W(n)\|$ decreases. By our choice, this improves the minimax value of the
 208 total tetrahelix.

209 This process can be carried out on both the Blue and Yellow helices (perhaps simulta-
 210 neously) until $W(n)$ is zero for both, finding a tetrahelix of improved overall minimax value
 211 at each step. So a tetrahelix is optimal only when $W(n) = 0$, and therefore when $D = 0$
 212 $B(n) = B'(n)$, all three axes are conincident. ■

213 Now that we have show that axes are conincident and parallel and that the pitches are
 214 the same for all helices, we can assert that any optimum tetrahelix can be generated with an
 215 equation for helices:

$$216 \quad (5) \quad V_{\text{triple}}(n, c) = \begin{bmatrix} r_c \cos(n\alpha + c2\pi/3 + \phi_c) \\ r_c \sin(n\alpha + c2\pi/3 + \phi_c) \\ \frac{d(n+c/3)}{3} \end{bmatrix}, \text{where: } c \in \{0, 1, 2\}$$

217 which would not be much more complicated if the axes where not coincident. Note that we
 218 have not yet show that the relationships of the radius r or the phase ϕ for the three helies, so
 219 we denoted them with a c subscript to show they are dependent on the color. In section 4 we
 220 give a more specific version of this formula which is optimal.

221 In principle in any three helices generated with (5) has at most nine distinct edge length
 222 classes. Each edge that connects two rails potentially has a longer length and shorter length
 223 we denote with a $+$ or $-$. So the classes are $\{RR, BB, YY, RB_+, RB_-, BY_+, BY_-, RY_+, RY_-\}$.
 224 If when projecting all vertices on the the z -axis, the interval defined by the z axis value of its
 225 endpoints contains no other vertices, we call it a *one-hop* edge, and if it does contain another
 226 vertex we call it a *two-hop* edge. Then there are 3 rail edges $\{RR, BB, YY\}$, 3 one-hop lengths
 227 $\{RB_-, BY_-, RY_-\}$ between each pair of 3 rails, and 3 two-hop lengths $\{RB_+, BY_+, RY_+\}$
 228 between each pair of 3 rails, where the two-hop length is at least the one-hop length. However,
 229 if we generate the three helices symmetrically with (5), many of these lengths will be the same.
 230 In fact, it is possible that there will be only two distinct such classes.

231 Now we show that an optimal tetrahelix has the same radii for all three helices. To do this
 232 exhibit a symmetric tetrahelix (not yet shown to be optimal) which happens to be a triple
 233 helix, that has the property that all rail edges are equal to all one-hop edges and all two-hop
 234 edges are equal. Observe that although we have not get given the formula for the radii of
 235 such a triple helix, we observe there are some values for r and α , and ϕ for which all the three
 236 helices are symmetrically and evenly spaced. Furthermore, we can choose these values such
 237 that the three rail edges are of length unity and so that the one-hop lengths are also all of
 238 length unity, and the two-hop lengths are slightly longer. We call such a tetrahelix a two-class

239 tetrahelix.

240 Now consider a tetrahelix in which the radius of one of the helices is different. By the
241 connections made in a tetrahelix, any increase to a radius increases both a one-hop and two-
242 hop distance, and any decrease likewise decreases two. Since there exists a tetrahelix which
243 has only two distinct classes of edge lengths, (the smaller being one-hop = rail, the larger
244 being the two-hop distance), the helix with a larger radius increases a longest edge without
245 increasing a shortest edges. Likewise, a helix with a smaller radius decreases a one-hop edge
246 without decreasing a two-hop edge. Therefore, a tetrahelix with different radii is not optimal
247 as some two-class tetrahelix generated by (5), and so it not optimal. We have not yet proved
248 that a two-class tetrahelix is optimal, but it suffices to show that there exist such a better
249 tetrahelix to show that different radii imply a suboptimal tetrahelix.

250 Because an optimal tetrhelix has equivalent radii and equivalent pitch for all three helices,
251 it has equivalent rail edge lengths. Likewise, there is a single rail angle ρ that represents the
252 rotation of two nodes connected by a single rail edge, and it is the same for all three rails.

253 Now that we have shown that any optimal tetrahelix vertices are on helices of the same
254 axes and pitch, we see that the vertices of any optimal tetrahelix will lie on a cylinder, or a
255 circle when axis dimension is projected out. Therefore it is reasonable to now speak of the
256 singular *radius r* of a tetrahelix as the radius of the cylinder. We can now go on to the harder
257 proof about where vertices occur along the z -axis.

258 We show that in fact the nodes must be distributed in even thirds along the z -axis, as in
259 fact they are in the regular BC helix.

260 Note that from the point of view of a single edge, we are on a slanted cylinder, when
261 $\rho \neq 0$. This means from its point of view a cross section is an ellipse. So we have to be very
262 careful in comparing lengths of edges relative to the tetrahedron, because a change in position
263 along the edge changes the length of a line, but in a complicated way depending on where it
264 is relative to the ellipse.

265 However, we have already shown the rail lengths are equal in any optimal tetrahelix.

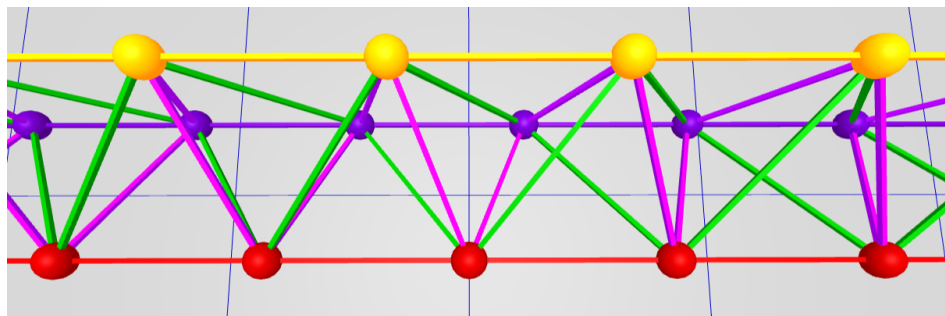


Figure 7. Equitetrabeam

266 Figure 7 shows the equitetrabeam, which is defined in section 6, but also conveniently
267 illustrates the one-hop and two-hop edge definitions. The green edges are the two-hop edges
268 and the purple edges are the one-hop edges. Note that the green edges are slightly longer
269 than the purple edges.

270 **Theorem 2.** *An optimal tetrahelix of any rail angle $\rho < \pi$ is a triple helix with all vertices
271 evenly spaced at $d/3$ intervals on the z axis. Any one tetrahedron in a tetrahelix has 1 rail
272 edge, 2 one-hop edges connected to the rail and 2 two-hop edges connected to the rail. The
273 edge opposite of the rail edge is a one-hop edge.*

274 *Proof.* Consider the tetrahelix in which the vertices are evenly spaced at $d/3$ intervals on
275 the z axis. Every edge is either a rail edge, or it makes one hop, or it makes two hops. All of
276 the one-hop edges are equal length. All of the two-hop edges are equal length.

277 Every vertex is connected to 4 non-rail edges. There is a one-hop edge in both the positive
278 and negative z direction. Likewise there is a two-hop edge in both the positive and negative
279 z direction. Let A be the set of edge lengths, which has only 3 members, represented by
280 $A = \{o, t, r\}$ for the one-hop, two-hop, and rail edge lengths.

281 Any attempt to move any rail in either z direction lengthens one two-hop edge to t' , where
282 $t' > t$ and shortens one one-hop edge $o' < o$. Let $B = \{o', t'\} \cup A$ be new edges. The minimax
283 of B is greater than the minimax of A since there is a single rail length which cannot be both
284 greater than t' and o' and less than t' and o' . Therefore, any optimal tetrahelix has all one-hop
285 edges between all rails equal to each other, and all two-hop edges equal to each other, and the
286 z distances between rails equal, and therefore $d/3$ from each other.

287 Note that based on [Theorem 2](#), there are only 3 possible lengths in an optimal tethrahelix,
288 and we are justified in classifying edge lengths as *rail*, *one-hop*, or *two-hop*. The one-hop edges
289 are the edges between rails that are closest on the z -axis, and the two-hop edges are those
290 that skip over a vertex.

291 In [section 4](#) have not yet investigated in the general case the relationships between α ,
292 r , ϕ and d in [\(5\)](#). However, we observe that when $\alpha = 0$, the helices are degenerate, having
293 curvature of 0, and we have the equitetrabeam.

294 Taking all of these results together, each helix in an optimal tetrahelix is congruent to the
295 others, shares an axis, is the same radius, and are evenly spaced axially. An optimal tetrahelix
296 is therefore a *triple helix*.

297 **4. Parameterizing Tetrahelices via Rail Angle.** We seek a formula to generate optimal
298 tetrahelices that accepts a parameter that allows us to design the tetrahelix conveniently.
299 Please refer back to [Figure 5](#). The pitch of the helix is an obvious choice, but is not defined
300 when the curvature is 0, an important special case. The radius or the axial distance between
301 two nodes on the same rail are possible choices, but perhaps the clearest choice is to build
302 formulae that takes as their input the “rail angle” ρ . We define ρ to be the angle formed in
303 the X,Y plane $\angle H(0,0)OH(0,1)$ projecting out the z axis and sighting along the positive z
304 axis. In other words, ρ controls how far a rail edge of a tetrahelix deviates from being parallel
305 with the axis, or the “twistiness” of the tetrahelix. We use the parameter $\chi = 1$ to indicate a
306 chirality of counter-clockwise, and $\chi = -1$ for clockwise.

307 The quantities ρ, r, d are related by the expression:

$$\begin{aligned} 308 \quad & 1^2 = d^2 + (2r \sin \rho/2)^2 \\ 309 \quad (6) \quad & d^2 = 1 - 4r^2(\sin \rho/2)^2 \\ 310 \quad & \end{aligned}$$

Checking the important special case of the BC helix, we find that this equation indeed holds true (treating d in this equation as $3h_{bc}$ as defined by Gray and Coxeter, that is, $d_{bc} = 3h_{bc}$, where they are using h for the axial height from one node to the next of a different color, but we use d to mean distance between nodes of the same color).

The rail angle ρ also has the meaning that $2\pi/\rho$ is the number of tetraheda in a full revolution of the helix.

In choosing ρ , one greatly constrains r and d , but does not completely determine both of them together, so we treat both as parameters.

320 Rewriting our formulation in terms of ρ :

$$H_{general}(\chi, n, c, \rho, d_\rho, r_\rho) = \begin{bmatrix} r_\rho \cos(\chi \cdot (n\rho + c(\rho + 2\pi)/3)) \\ r_\rho \sin(\chi \cdot (n\rho + c(\rho + 2\pi)/3)) \\ d_\rho(n + c/3) \end{bmatrix}$$

where: $1 = d_\rho^2 + 4r_\rho^2(\sin \rho/2)^2$
 $\chi \in \{-1, 1\}$

H_{general} forces the user to select three values: ρ , r_ρ , and d_ρ satisfying (6). Note that when $\rho = 0$ then $d_\rho = 1$, but r_ρ is not determined by (6).

Theorem 3. The tetrahelices generated by H_{general} are optimal in terms of minimum maximum ratio of member length when r_ρ is chosen so that the length of the one-hop edge is equal to the rail length.

329 *Proof.* This is proved by a minimax argument.

330 By [Theorem 2](#), we can compute the (at most) three edge-lengths of an optimal tetrahelix
 331 by formula universally quantified by n and c :

rail = $dist(H_{general}(n, c, \rho, d_\rho, r_\rho), H_{general}(n + 1, c, \rho, d_\rho, r_\rho)) = 1$
 one-hop = $dist(H_{general}(n, c, \rho, d_\rho, r_\rho), H_{general}(n, c + 1, \rho, d_\rho, r_\rho))$
 two-hop = $dist(H_{general}(n, c, \rho, d_\rho, r_\rho), H_{general}(n, c + 2, \rho, d_\rho, r_\rho))$

337 where $dist$ is the Cartesian distance function.

338 one-hop = $dist(H_{general}(n, c, \rho, d_\rho), H_{general}(n, c + 1, \rho, d_\rho), r_\rho)$

339 one-hop = $\sqrt{\frac{d_\rho^2}{9} + r_\rho^2(\sin^2(\rho/3 + \frac{2\pi}{3}) + (1 - \cos(\rho/3 + \frac{2\pi}{3}))^2)}$

340 but: $d_\rho^2 = 1 - 4r_\rho^2(\sin(\rho/2)^2)$...so we substitute:

341 one-hop = $\sqrt{\frac{1}{9} + r_\rho^2(-\frac{4(\sin^2(\rho/2))}{9} + \sin^2(\rho/3 + \frac{2\pi}{3}) + (1 - \cos(\rho/3 + \frac{2\pi}{3}))^2)}$

342

344 By similar algebra and trigonometry:

345 two-hop = $\sqrt{\frac{4}{9} + r_\rho^2(-\frac{16(\sin^2(\rho/2))}{9} + \sin^2(2\rho/3 + \frac{4\pi}{3}) + (1 - \cos(2\rho/3 + \frac{4\pi}{3}))^2)}$

346

348 We would really like to know the partial derivative of the two-hop - one-hop with respect
349 to the radius to be able to understand how to choose the radius to form the minimimax
350 optimum.

351 Let:

352 $f_\rho = -\frac{4(\sin^2(\rho/2))}{9}$

353

354 $g_\rho = -\frac{16(\sin^2(\rho/2))}{9}$

355 $j_\rho = \sin^2(\rho/3 + \frac{2\pi}{3}) + (1 - \cos(\rho/3 + \frac{2\pi}{3}))^2$

356

357 $k_\rho = (\sin^2(2\rho/3 + \frac{4\pi}{3}) + (1 - \cos(2\rho/3 + \frac{4\pi}{3}))^2)$

358 Then:

359 two-hop - one-hop = $\sqrt{\frac{4}{9} + r_\rho^2(g_\rho + j_\rho)} - \sqrt{\frac{1}{9} + r_\rho^2(f_\rho + k_\rho)}$

361 By graph inspection using Mathematica, we see the partial derivative of this with respect
362 to radius r_ρ is always negative. Since the partial derivative of two-hop - one-hop with respect
363 to the radius r_ρ is negative up until ρ_{bc} where it is 0, we optimize the overall minimimax distance
364 by choosing the largest radius up until one-hop = 1, the rail-edge length.

365 Therefore we decrease the minimimax length of the whole system as we increase the radius
366 up to the point that the shorter, one-hop distance is equal to the rail-length (1). Therefore,

367 to optimize the whole system so long as $\rho \leq \rho_{bc}$, we equate one-hop to 1 to find the optimum
 368 radius:

$$369 \quad 1 = \sqrt{\frac{1}{9} + r_{opt}^2 \left(-\frac{4(\sin^2(\rho/2))}{9} + \sin^2(\rho/3 + \frac{2\pi}{3}) + (1 - \cos(\rho/3 + \frac{2\pi}{3}))^2 \right)}$$

$$370 \quad (8) \quad r_{opt} = \frac{2}{\sqrt{\frac{9}{2} \cdot (\sqrt{3}\sin(\rho/3) + \cos(\rho/3)) + \cos(\rho) + 8}}$$

371

373 We can now give a formula for d_{opt} computed from ρ, r_{opt} via the rail angle equation (6):

$$374 \quad d_{opt}^2 = 1 - 4 \left(\frac{2}{\sqrt{\frac{9}{2} \cdot (\sqrt{3}\sin(\rho/3) + \cos(\rho/3)) + \cos(\rho) + 8}} \right)^2 (\sin \rho/2)^2$$

$$375 \quad d_{opt}^2 = 1 - \frac{16(\sin \rho/2)^2}{9(\sqrt{3}\sin(\rho/3) + \cos(\rho/3)) + \cos(\rho) + 8}$$

$$376 \quad (9) \quad d_{opt} = \sqrt{1 - \frac{16 \sin^2(\rho/2)}{\cos(\rho) + 9(\sqrt{3}\sin(\rho/3) + \cos(\rho/3)) + 8}}$$

377

379 Thus, by computing r_{opt} and d_{opt} as a function of ρ from this equation, we can construct
 380 minimax optimal tetrahelix for an $0 \leq \rho \leq \rho_{bc}$. ■

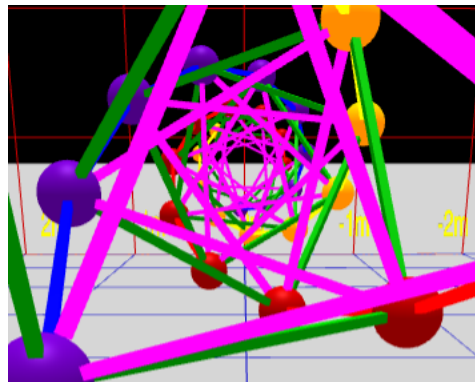


Figure 8. Axial view of a BC-Helix

381 **5. The Inradius.** Since the axes are parallel, we may define the *inradius*, represented by
 382 the letter i , of a tetrahelix to be the radius of the largest cylinder parallel to this axis that is
 383 surrounded by each tetrahelix and penetrated by no edge.

384 If we look down the axis of an optimal tetrahelix as shown in Figure 8, it happens that
 385 only one of the one-hop edges (rendered in purple in our software) comes closest to the axis. In

386 other words, they define the radius of the incircle of the projection, or the radius of a cylinder
 387 that would just fit inside the tetrahelix. A formula for the inradius of the tetrahelix is useful
 388 if you are designing it as a structure that bears something internally, such as a firehose, a
 389 pipe, or a ladder for a human. The inradius $r_{in}(\rho)$ of an optimal tetrahelix is a remarkably
 390 simple function of the radius r and the rail angle ρ :

$$391 \quad (10) \quad r_{in}(\rho) = r \sin \frac{\pi - \rho}{6}$$

392 Which can be seen from the trigonometry of a diagram of the projected one-hop edges con-
 393 necting four sequentially numbered vertices:

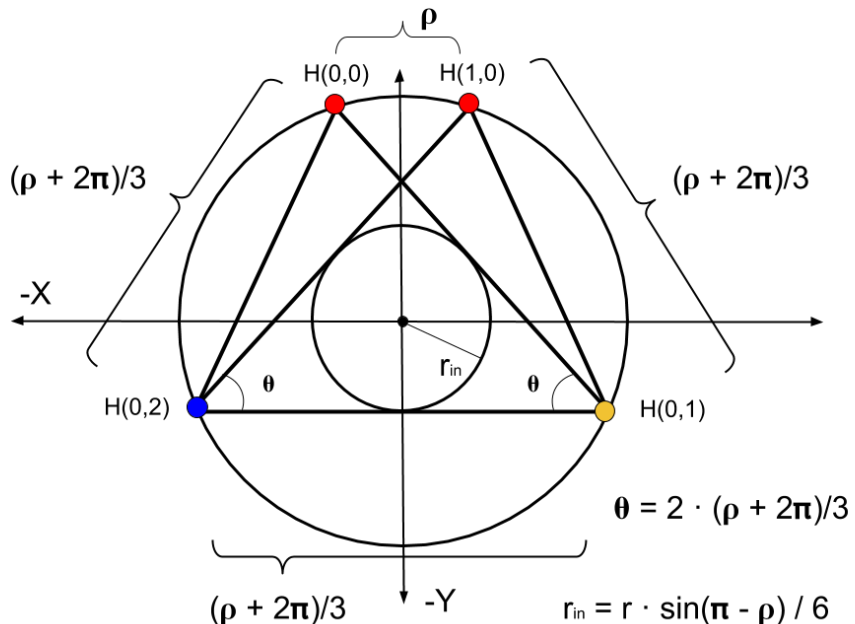


Figure 9. General One-hop Projection Diagram

394 From this equation with the help of symbolic computation we observe that inradius of the
 395 BC helix of unit rail length is $r_{in}(\rho_{bc}) = \frac{3}{10\sqrt{2}} \approx 0.21$.

396 **6. The Equitetrabeam.** Just as $H_{general}$ constructs the BC helix (with careful and non-
 397 obvious choices of parameters) which is an important special case due to its regularity, it
 398 constructs an additional special (degenerate) case when the rail angle $\rho = 0$ and $d = 1$ (the
 399 edgelength), where the cross sectional area is an equilateral triangle of unchanging orientation,
 400 as shown in [Figure 7](#) and at the rear of [Figure 3](#). We call this the *equitetrabeam*. It is not
 401 possible to generate an equitetrabeam from (1) without the split into three rails introduced
 402 by (2) and completed in (7).

403 **Corollary 4.** *The equitetrabeam with minimal maximal edge ratio is produced
 404 by H_{general} when $r = \sqrt{\frac{8}{27}}$.*

405 **Proof.** Choosing $d = 1$ and $\rho = 0$ we use Equation (8) to find the radius of optimal
 406 minimax difference.

407 Substituting into (7):

$$408 \quad \text{one-hop} = \sqrt{\frac{1}{9} + 3r^2}$$

409

410 Then:

$$411 \quad 1 = \sqrt{\frac{1}{9} + 3r^2} \quad \text{solved by...}$$

$$412 \quad r = \sqrt{\frac{8}{27}} \quad \approx 0.54$$

413

414 This radius¹ produces a two-hop rail length of $\frac{2}{\sqrt{3}}$. The difference between this and 1 is
 415 $\approx 15.47\%$. The inradius of the equitetrabeam of unit rail length from both Equation (10) and
 416 the fact that the inradius of an equilateral triangle is half the circumradius is $\sqrt{\frac{8}{27}}/2$, or $\frac{\sqrt{6}}{9}$.

417 In Figure 3, the furthest tetrahelix is the optimal equitetrabeam. Figure 7 is a closeup of
 418 an equitetrabeam.

419 To the extent that we value tetrabeams (that is, tetrahelices with a rail angle of 0, and
 420 therefore zero curvature and curvature) as mathematical or engineering objects, we have
 421 motivated the development of H_{general} as a transformation of $V(n)$ defined by Equation (1)
 422 from Gray and Coxeter. It is difficult to see how the $V(n)$ formulation could ever give rise
 423 to a continuum producing the tetrabeam, since setting the angle in that equation to zero can
 424 produce only collinear points.

425 The equitetrabeam may possibly be a novel construction. The fact that 6 members meet
 426 in a single point would have been a manufacturing disadvantage that may have dissuaded
 427 structural engineers from using this geometry. However, the advent of additive manufacturing,
 428 such a 3D printing, and the invention of two distinct concentric multimember joints[15, 7] has
 429 improved that situation.

430 Note that the equitetrabeam has chirality, which becomes important in our attempt to
 431 build a continuum of tetrahelices.

432 **7. An Untwisted Continuum.** We observe that Equations (8) and (9) compute r_{opt} and
 433 d_{opt} which create an optimal tetrahelix for any rail angle ρ between 0, which gives the equi-
 434 tetrabeam and $\rho_{bc} \approx 35.43^\circ$, which gives the BC helix.

¹Another interesting but non-optimal solution is derived by setting $(\text{one-hop} + \text{two-hop})/2 = 1$, occurs at $r = \sqrt{35}/4$ which produces three length classes of $11/12, 12/12, 13/12$.

437 Because the equitetrabeam which has a rail angle of 0 still has chirality, that is, one still
 438 must decide to connect the one-hop edge to the clockwise or the counter-clockwise node, it
 439 is not possible to build a smooth continuum where ρ transitions from positive to negative
 440 which remains optimal. One can use a negative ρ in $H_{general}$ but it does not produce minimax
 441 optimal tetrahelices. In other words, untwisting a counter-clockwise tetrahelix to rail angle 0
 442 and then going even further does produce a clockwise tetrahelix, but one in which the one-hop
 443 and two-hop lengths in the wrong places (that is, two-hop becomes shorter than one-hop.)
 444 Likewise, $\rho > \rho_{bc}$ generates a tetrahelix, but minimax optimality is not guaranteed by $H_{general}$.

445 The pitch of a helix (see (4), for a fixed z -axis travel d , is trivial. However, if one is
 446 computing z -axis travel from (9) the pitch is not simple. It increases monotonically and
 447 smoothly with decreasing ρ , so Equation (4) can be easily solved numerically with a Newton-
 448 Raphson solver, as we do on our website. For a pitch at least $p \geq \frac{3\sqrt{2}\pi}{\sqrt{5}\rho_{bc}} \approx 9.64$, using (9)
 449 produces minimax optimal tetrahelices.

450 In this way a rail angle can be chosen for any desired (sufficiently large) pitch, yield the
 451 optimum radius, one-hop, and two-hop lengths an engineer needs to construct a physical
 452 structure.

453 The curvature of a rail helix is formally given by:

$$454 \quad (11) \quad \frac{|r_\rho|}{r_\rho^2 + (d_\rho/\rho)^2}$$

455 which goes to 0 as ρ approaches 0 (the equitetrabeam.) As ρ increase up to ρ_{bc} the curvature
 456 increases smoothly until the BC Helix is reached.

457 Perhaps surprisingly, the optimal untwisting is accomplished only by changing the length
 458 of the two-hop member, leaving the one-hop member and rail length equivalent within this
 459 continuum.² However, it should be noted that an engineer or architect may also use $H_{general}$
 460 directly and interactively, and that minimax length optimality is a mathematical starting point
 461 rather than the final word on the beauty and utility of physical structures. For example, a
 462 structural engineer might increase radius past optimality in order to resist buckling.

463 If an equitetrabeam were actually used as a beam, an engineer might start with the
 464 optimal tetrabeam and dilate it in one dimension to “deepen” the beam. Similarly, simple
 465 length changes curve the equitetrabeam into an “arch”. The “colored” approach of (7) exposes
 466 these possibilities more than the approach of (1).

467 Trusses and space frames remain an important design field in mechanical and structural
 468 engineering[10], including deployable and moving trusses[2].

469 **8. Utility for Robotics.** Starting twenty years ago, Sanderson[14], Hamlin,[8], Lee[9], and
 470 others created a style of robotics based on changing the lengths of members joined at the
 471 center of a joint, thereby creating a connection to pure geometry. More recently NASA has
 472 experimented with tensegrities[1], a different point in the same design spectrum. These fields
 473 create a need to explore the notion of geometries changing over time, not generally considered
 474 directly by pure geometry.

²Before deriving Equation (8), we created a continuum by using a linear interpolation between the optimal radius for the Equitetrabeam and the BC Helix. This minimax optimum of this simpler approach was at most 1% worse than the optimum computed by (8).

475 As suggested by Buckminster Fuller, the most convenient geometries to consider are those
476 that have regular member lengths, in order to facilitate the inexpensive manufacture and
477 construction of the robot. In a plane, the octet truss[4] is such a geometry, but in a line, the
478 Boerdijk–Coxeter helix is a regular structure.

479 However, a robot must move, and so it is interesting to consider the transmutations of
480 these geometries, which was in fact the motivation for creating the equitetrabream.

481 **Theorem 5.** *By changing only the length of the longer members that connect two distinct*
482 *rails (the two-hop members), we can dynamically untwist a tetrobot forming the Boerdijk–*
483 *Coxeter configuration into the equitetrabream which rests flat on the plane.*

484 **Proof.** Proof by our computer program that does this using Equation (7) applied to the
485 7-tet Tetrobot/Glussbot.

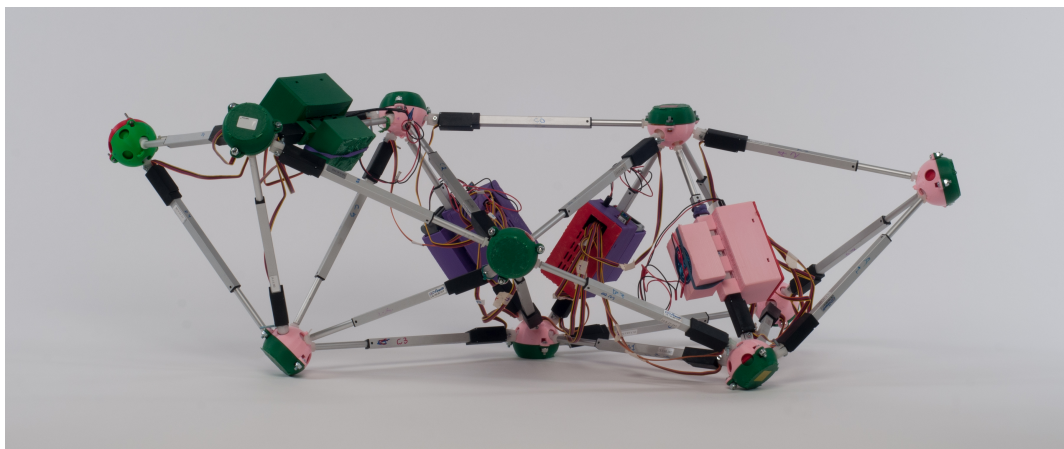


Figure 10. *Glussbot in relaxed, or BC helix configuration*

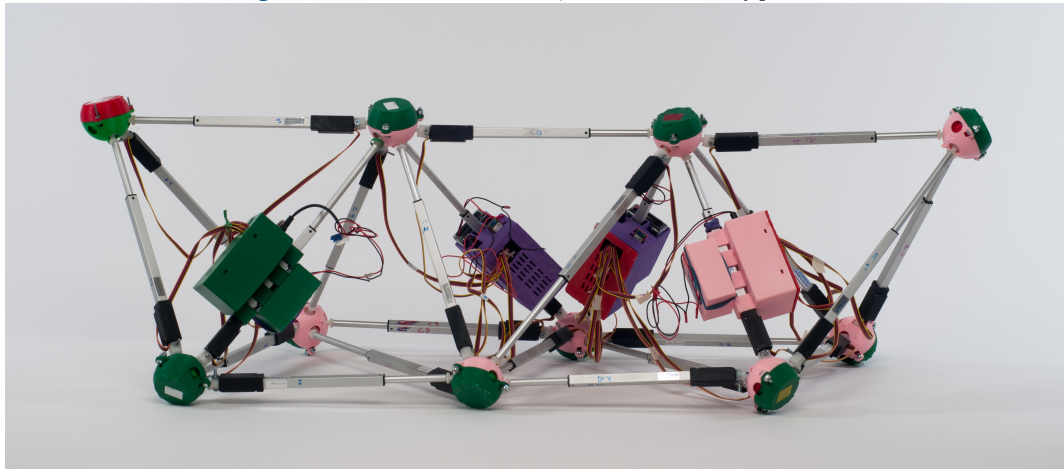


Figure 11. *The Equitetraabream: Fully Untwisted Glussbot in Hexapod Configuration*

486 By untwisting the tetrahelix so that it has a planar surface resting on the ground, we may
487 consider each vertex touching the ground a foot or pseudopod. A robot can thus become a

488 hexapod or n -pod robot, and the already well-developed approaches to hexapod gaits may be
489 applied to make the robot walk or crawl.

490 **9. Conclusion.** The BC Helix is the end point of a continuum of tetrahelices, the other end
491 point being an untwisted tetrahelix with equilateral cross section, constructed by changing the
492 length of only those members crossing the outside rails after hopping over the nearest vertex.
493 Under the condition of minimum maximum length ratios of all members in the system, all
494 such tetrahelices have vertices evenly spaced along the axis generated by a simple equation
495 and are in fact triple helices. A machine, such as a robot or a variable-geometry truss, that
496 can change the length of its members can thus twist and untwist itself by changing the length
497 of the appropriate members to achieve any point in the continuum. With a numeric solution,
498 a design may choose a rotation angle and member lengths to obtain a desired pitch.

499 **10. Contact and Getting Involved.** The Gluss Project <http://pubinv.github.io/gluss/> is
500 part of Public Invention <https://pubinv.github.io/PubInv/>, a free-libre, open-source research,
501 hardware, and software project that welcomes volunteers. It is our goal to organize projects for
502 the benefit of all humanity without seeking profit or intellectual property. To assist, contact
503 read.robert@gmail.com.

504

REFERENCES

- 505 [1] *NTRT - NASA Tensegrity Robotics Toolkit.* <https://ti.arc.nasa.gov/tech/asr/intelligent-robotics/tensegrity/ntrt/>. Accessed: 2016-09-13.
506
507 [2] J. CLAYPOOL, *Readily configured and reconfigured structural trusses based on tetrahedrons as modules*,
508 Sept. 18 2012, <https://www.google.com/patents/US8266864>. US Patent 8,266,864.
509
510 [3] H. COXETER ET AL., *The simplicial helix and the equation $\tan(n \theta) = n \tan(\theta)$* , Canad. Math. Bull, 28
511 (1985), pp. 385–393.
512
513 [4] R. FULLER, *Synergetic building construction*, May 30 1961, <https://www.google.com/patents/US2986241>.
514 US Patent 2,986,241.
515
516 [5] R. FULLER AND E. APPLEWHITE, *Synergetics: explorations in the geometry of thinking*, Macmillan, 1982,
517 <https://books.google.com/books?id=G8baAAAAMAAJ>.
518
519 [6] R. W. GRAY, *Tetrahelix data*. <http://www.rwgrayprojects.com/rbfnotes/helix/helix01.html>, <http://www.rwgrayprojects.com/rbfnotes/helix/helix01.html> (accessed Accessed: 2017-04-08).
520
521 [7] G. J. HAMLIN AND A. C. SANDERSON, *A novel concentric multilink spherical joint with parallel robotics*
522 *applications*, in Proceedings of the 1994 IEEE International Conference on Robotics and Automation,
523 May 1994, pp. 1267–1272 vol.2, <https://doi.org/10.1109/ROBOT.1994.351313>.
524
525 [8] G. J. HAMLIN AND A. C. SANDERSON, *Tetrobot: A Modular Approach to Reconfigurable Parallel*
526 *Robotics*, Springer Science & Business Media, 2013, <https://play.google.com/store/books/details?id=izrSBwAAQBAJ> (accessed 2017-04-08).
527
528 [9] W. H. LEE AND A. C. SANDERSON, *Dynamic rolling locomotion and control of modular robots*, IEEE
529 Transactions on robotics and automation, 18 (2002), pp. 32–41.
530
531 [10] M. MIKULAS AND R. CRAWFORD, *Sequentially deployable maneuverable tetrahedral beam*, Dec. 10 1985,
532 <https://www.google.com/patents/US4557097>. US Patent 4,557,097.
533
534 [11] R. L. READ, *Gluss = Slug + Truss*. Unpublished preprint, <https://github.com/PubInv/gluss/blob/gh-pages/doc/Gluss.pdf> (accessed 2016-10-27).
535
536 [12] R. L. READ, *Untwisting the tetrahelix website*. <https://pubinv.github.io/tetrahelix/>, <https://pubinv.github.io/tetrahelix/> (accessed 2017-04-08).
537
538 [13] G. SADLER, F. FANG, J. KOVACS, AND K. IRWIN, *Periodic modification of the Boerdijk-Coxeter helix*
539 (*tetrahelix*), arXiv preprint arXiv:1302.1174, (2013), <https://arxiv.org/abs/1302.1174>.

- 533 [14] A. C. SANDERSON, *Modular robotics: Design and examples*, in Emerging Technologies and Factory Au-
534 tomation, 1996. EFTA'96. Proceedings., 1996 IEEE Conference on, vol. 2, IEEE, 1996, pp. 460–466.
535 [15] S. SONG, D. KWON, AND W. KIM, *Spherical joint for coupling three or more links together at one point*,
536 May 27 2003, <http://www.google.com/patents/US6568871>. US Patent 6,568,871.